Combined glucose-dependent insulinotropic polypeptide receptor and glucagon-like peptide-1 receptor agonism attenuates atherosclerosis severity in APOE*3-Leiden.CETP mice

van Eenige, Robin; Ying, Zhixiong; Tramper, Naomi; Wiebing, Vera; Siraj, Zohor; de Boer, Jan Freark; Lambooij, Joost M.; Guigas, Bruno; Qu, Hongchang; Coskun, Tamer

Published in:
Atherosclerosis

DOI:
10.1016/j.atherosclerosis.2023.03.016

Atherosclerosis 372 (2023) 19–31

Contents lists available at ScienceDirect

Atherosclerosis

journal homepage: www.elsevier.com/locate/atherosclerosis

Combined glucose-dependent insulinotropic polypeptide receptor and glucagon-like peptide-1 receptor agonism attenuates atherosclerosis severity in APOE*3-Leiden.CETP mice

Robin van Eenige [a,b,1], Zhixiong Ying [a,b,1], Naomi Tramper [a,b], Vera Wiebing [a,b], Zohor Siraj [a,b], Jan Freark de Boer [c], Joost M. Lambooij [d,e], Bruno Guigas [d], Hongchang Qu [f], Tamer Coskun [f], Mariëtte R. Boon [a,b], Patrick C.N. Rensen [a,b], Sander Kooijman [a,b,*]

[a] Division of Endocrinology, Department of Medicine, Leiden University Medical Center, Leiden, the Netherlands
[b] Einthoven Laboratory for Experimental Vascular Medicine, Leiden University Medical Center, Leiden, the Netherlands
[c] Departments of Pediatrics and Laboratory Medicine, University of Groningen, University Medical Center Groningen, Groningen, the Netherlands
[d] Department of Parasitology, Leiden University Medical Center, Leiden, the Netherlands
[e] Department of Cell and Chemical Biology, Leiden University Medical Center, Leiden, the Netherlands
[f] Lilly Research Laboratories, Lilly Corporate Center, Indianapolis, IN, United States

HIGHLIGHTS

- Combined GIPR/GLP1R agonism attenuates atherosclerosis severity.
- Less systemic low-grade inflammation and lower plasma triglyceride levels underly the reduced atherosclerosis severity.
- The lowered plasma triglyceride levels upon combined GIPR/GLP1R agonism are the result of higher VLDL turnover.

GRAPHICAL ABSTRACT

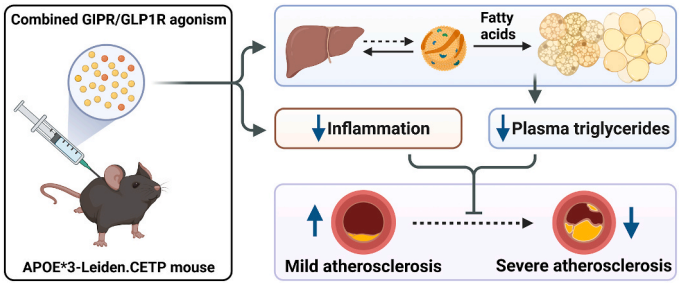

ARTICLE INFO

Keywords:
Adipose tissue
Atherosclerosis
Cardiovascular disease
Glucagon-like peptide-1
Glucose-dependent insulinotropic polypeptide
Lipoprotein metabolism

ABSTRACT

Background and aims: Combined agonism of the glucose-dependent insulinotropic polypeptide receptor (GIPR) and the glucagon-like peptide-1 receptor (GLP1R) is superior to single GLP1R agonism in terms of glycemic control and lowering body weight in individuals with obesity and with or without type 2 diabetes mellitus. As both GIPR and GLP1R signaling have also been implicated in improving inflammatory responses and lipid handling, two crucial players in atherosclerosis development, here we aimed to investigate the effects of combined GIPR/GLP1R agonism in APOE*3-Leiden.CETP mice, a well-established mouse model for human-like lipoprotein metabolism and atherosclerosis development.
Methods: Female APOE*3-Leiden.CETP mice were fed a Western-type diet (containing 16% fat and 0.15% cholesterol) to induce dyslipidemia, and received subcutaneous injections with either vehicle, a GIPR agonist

* Corresponding author. Albinusdreef 2, 2333ZA, P.O. Box 9600, 2300 RC, Leiden, the Netherlands.
E-mail addresses: r.van_eenige@lumc.nl (R. van Eenige), s.kooijman@lumc.nl (S. Kooijman).
[1] These authors contributed equally to this work.

https://doi.org/10.1016/j.atherosclerosis.2023.03.016
Received 20 September 2022; Received in revised form 21 March 2023; Accepted 22 March 2023
Available online 28 March 2023

(GIPFA-085), a GLP1R agonist (GLP-140) or both agonists. In the aortic root area, atherosclerosis development was assessed.
Results: Combined GIPR/GLP1R agonism attenuated the development of severe atherosclerotic lesions, while single treatments only showed non-significant improvements. Mechanistically, combined GIPR/GLP1R agonism decreased markers of systemic low-grade inflammation. In addition, combined GIPR/GLP1R agonism markedly lowered plasma triglyceride (TG) levels as explained by reduced hepatic very-low-density lipoprotein (VLDL)-TG production as well as increased TG-derived fatty acid uptake by brown and white adipose tissue which was coupled to enhanced hepatic uptake of core VLDL remnants.
Conclusions: Combined GIPR/GLP1R agonism attenuates atherosclerosis severity by diminishing inflammation and increasing VLDL turnover. We anticipate that combined GIPR/GLP1R agonism is a promising strategy to lower cardiometabolic risk in humans.

1. Introduction

Obesity has reached epidemic proportions, and strongly increases the risk for diseases such as type 2 diabetes mellitus (T2DM) and atherosclerotic cardiovascular disease (asCVD). Glucagon-like peptide-1 (GLP1) is an incretin hormone secreted by enteroendocrine L-cells upon nutrient ingestion, which enhances the glucose-induced release of insulin by pancreatic β-cells as part of the so-called incretin response. At supraphysiological levels, GLP1 receptor (GLP1R) agonism additionally reduces appetite, delays gastric emptying, lowers body weight, and attenuates inflammation [1–3]. For these reasons, GLP1R agonists are currently used in the clinic for the treatment of T2DM [4] and obesity (*i.e.* liraglutide and semaglutide) [5].

Glucose-dependent insulinotropic polypeptide (GIP) is another incretin hormone that is secreted by enteroendocrine K-cells in response to nutrient ingestion. GIP has also been implicated in regulation of satiety and body weight [6,7], at least in part via mechanisms different from GLP1R agonism [6,8]. Therefore, it was hypothesized that GIP receptor (GIPR) agonism might complement GLP1R agonism with regard to its insulinotropic and weight-lowering effects. Indeed, co-infusion of both incretins resulted in additive effects on pancreatic β-cell responses [9], and treatment with the GIPR and GLP1R agonist NNC0090-2746 (RG7697) or tirzepatide (LY3298176; Mounjaro) showed superior glycemic control and weight loss in patients with T2DM, compared to single GLP1R agonism [10–12]. In addition, tirzepatide was recently shown to induce a marked loss of body weight of 22.5% (23.6 kg) on average in obese, non-diabetic participants after 72 weeks of treatment in the recent SURMOUNT-1 trial [13], thereby approaching the effects of bariatric surgery [14].

It is anticipated that at least part of the insulin-sensitizing effect of combined GIPR/GLP1R agonism is weight-independent and the result of improved (postprandial) lipid handling by adipose tissue [1,8]. Combined with the observation that both GIPR and GLP1R agonists are also potent suppressors of inflammatory responses [1,15], this raises the question whether combined GIPR/GLP1R agonism also protects against asCVD for which dyslipidemia and inflammation are major risk factors. To address this question, we treated APOE*3-Leiden.CETP mice, a well-established mouse model for human-like lipoprotein metabolism and atherosclerosis development [16], with either a GIPR agonist, a GLP1R agonist, or the combination thereof to show that combined GIPR/GLP1R treatment attenuates systemic low-grade inflammation, accelerates the turnover of atherogenic lipoproteins and reduces atherosclerotic lesion severity.

2. Materials and methods

2.1. Animals and intervention

All mouse experiments were performed in accordance with the Institute for Laboratory Animal Research Guide for the Care and Use of Laboratory Animals and had received approval from the National Committee for Animal Experimentation of the Netherlands ("Centrale Commissie Dierproeven"). Homozygous human cholesteryl ester transfer protein (CETP) transgenic mice were crossbred with hemizygous APOE*3-Leiden mice to generate APOE*3-Leiden.CETP mice as detailed earlier [17]. Given that only female APOE*3-Leiden.CETP mice develop a sufficiently high cholesterol level in response to dietary cholesterol to promote atherosclerosis development, female mice (9–14 weeks of age) were used and were group housed in conventional cages under standard conditions at 22 °C, with a 12 h:12 h light:dark cycle (lights on at 7:00 a.m. clock time) and *ad libitum* access to water and a Western-type diet containing 16% fat (15% cocoa butter and 1% corn oil) and 0.15% cholesterol (Diet T; Sniff Spezialdiäten GmbH). After 3–4 weeks, the mice were divided over four treatment groups that were balanced for age, body weight, body composition and plasma triglycerides (TG), total cholesterol (TC), high-density lipoprotein-cholesterol (HDL-C) and non-HDL-C using RandoMice version 1.0.9 [18].

In experiment 1, mice were treated every other day via subcutaneous injection with a GIPR agonist (GIPFA-085; 300 nmol · kg^{-1}), a GLP1R agonist (GLP-140; 30 nmol · kg^{-1}), a combination of both agonists at these doses, or vehicle (0.02% Tween-80/20 mM Tris/HCl at pH 8.0) (n=16 per group) to primarily study effects on atherosclerosis development. Body weight and body composition were determined at regular intervals, as was food intake. 4-h fasted tail vein blood was collected at baseline and after 4, 8 and 10 weeks of treatment. Fecal samples were collected from the bedding of each home cage in the eighth week of intervention. Mice were killed after the last blood sampling for the collection of organs and tissues for further analyses.

In experiment 2, mice were treated daily with the GIPR agonist, the GLP1R agonist, the combination of both agonists or vehicle (n=8 per group). Unfasted tail vein blood was collected after two weeks for flow cytometry analysis. After four weeks of treatment, very-low-density lipoprotein (VLDL) production was assessed in 4-h fasted mice.

In experiment 3, mice were treated daily with the GIPR agonist, the GLP1R agonist, the combination of both agonists or vehicle (n=8 per group). Body weight and body composition were determined at regular intervals. Mice were individually housed in metabolic home cages for indirect calorimetry during the third week of treatment. After four weeks of treatment, VLDL plasma decay and organ uptake was assessed in 4-h fasted mice.

2.2. Peptide synthesis and in vitro characterization

The GIPR agonist GIPFA-085 and the GLP1R agonist GLP-140 were synthesized at Eli Lilly and Company. Functional activity of GIPFA-085 and GLP-140 was determined using cAMP formation assays in the absence of serum albumin in HEK-293 clonal cell lines expressing murine GIPR or murine GLP1R as previously described [19]. Peptide sequences and functional activity are presented in Suppl Tables S1 and S2. The *in vivo* pharmacokinetic and pharmacodynamic properties of the agonists have been described previously [19,20].

2.3. Body weight, body composition and food intake

Body weight was determined by placing the mouse on a regular

weighing scale, and body composition was determined using an EchoMRI-100 (EchoMRI) (experiments 1 and 3). Food intake was determined every other day by weighing the food and dividing by the number of mice per cage to express the data as cumulative food intake in gram per mouse (experiment 1).

2.4. Plasma lipid and glucose levels and lipoprotein profiles

Plasma (experiment 1) was obtained for the colorimetric measurement of TGs (10166588130; Roche Diagnostics), TC (11489232216; Roche Diagnostics) and glucose (10786, HUMAN). ApoB-containing lipoproteins were precipitated from plasma by addition of 20% polyethylene glycol (PEG)6000 (Sigma-Aldrich) in 200 mM glycine buffer (pH 10), after which HDL-C was determined in the supernatant. Non-HDL-C was calculated by subtracting HDL-C from TC. Lipoprotein fractions were generated from pooled plasma samples (equal plasma volumes per mouse in each group) by fast protein liquid chromatography (FPLC) using a Superose 6 column (Cytiva), to determine TG, cholesterol and phospholipid (3009; Instruchemie) profiles. In plasma obtained from heart puncture blood, insulin levels were determined using an Ultra Sensitive Mouse Insulin ELISA Kit (90080, Crystal Chem), which, together with the plasma glucose level, was used to calculate the homeostatic model assessment for insulin resistance (HOMA-IR) using the formula: glucose level (mM) · insulin level (μU/mL) · 22.5^{-1}.

2.5. Hepatic lipid content

Lipids were extracted from snap-frozen liver tissue (experiment 1, n=8 per group) according to a modified protocol of Bligh and Dyer [21]. Briefly, samples (approx. 50 mg) were homogenized in 10 μL CH_3OH per mg tissue. 45 μL homogenate was mixed with 1,800 μL cold CH_3OH:$CHCl_3$ (1:3 v · v^{-1}) by vigorous vortexing, and subsequently centrifuged (15 min; 20,000 · g; room temperature). The organic phase was dried under a gentle stream of nitrogen and dissolved in 100 μL 2% Triton X-100 in $CHCl_3$ to be dried again and dissolved in 100 μL H_2O. Colorimetric assays were used to determine TGs (10166588130; Roche Diagnostics), TC (11489232216; Roche Diagnostics), and phospholipids (3009; InstruChemie); lipid content was expressed as nmol per whole liver.

2.6. Atherosclerosis quantification

Hearts (experiment 1) were fixated in 4% paraformaldehyde, dehydrated, embedded in paraffin and cross-sectioned (5 μm) throughout the aortic root area. Cross-sections were stained with haematoxylin-phloxine-saffron to quantify atherosclerotic lesion area as described before [22]. Lesions were categorized as mild lesions (type I-III) or severe lesions (type IV-V) according to the description of Wong et al. [23], which was based on the guidelines of the American Heart Association adapted for mice. Collagen was stained with 0.1% Sirius Red in picric acid (1A280; Chroma; 1 h, room temperature). Cross-sections were treated with 0.3% H_2O_2 (10 min, room temperature) to block endogenous peroxidases, immersed in boiling citrate buffer (10 min) for antigen retrieval and subsequently stained using rat monoclonal anti-MAC-3 antibody (550292; BD Pharmingen; 1:1000, overnight, 4 °C) and Vector ImmPRESS® anti-rat (MP-7444; Vector Laboratories; 30 min, room temperature), or mouse monoclonal anti-actin antibody (M0851; Dako; 1:500, overnight, 4 °C) and DAKO EnVision™ anti-mouse (K4001; Dako; 30 min, room temperature), and visualized after incubation with 3,3′ diaminobenzidine (DAB; K3468; Dako; ~6 min, room temperature). ImageJ software (version 1.52a; National Institutes of Health) was used to quantify atherosclerotic lesion area, as well as macrophage, smooth muscle cell and collagen content.

2.7. Plasma levels of adhesion molecules

Intercellular adhesion molecule-1 (ICAM-1) and vascular cell adhesion molecule-1 (VCAM-1) were determined in plasma samples obtained after 10 weeks of treatment (experiment 1) by ELISA using manufacturer's protocols (MIC100 and MVC00, respectively; R&D Systems).

2.8. Gene expression analysis

Total RNA was isolated from snap-frozen liver samples (approx. 30–50 mg; n=8 per group of experiment 1) with TriPure RNA Isolation Reagent (Roche Diagnostics) following manufacturer's protocol. Of each sample, 1 μg RNA was used for cDNA synthesis using Moloney murine leukemia virus reverse transcriptase (M-MLV RT; Promega) following manufacturer's protocol. Quantitative real-time PCR was performed using GoTaq® qPCR Master Mix (A6002; Promega) with a Bio-Rad CFX96 Touch™ Real-Time PCR Detection System. mRNA expression levels were normalized to ribosomal protein lateral stalk subunit P0 (*Rplp0*) mRNA expression and expressed as fold change *vs* vehicle controls using the $2^{-\Delta\Delta CT}$ method. Primer sequences are presented in Table S3.

2.9. Fecal energy, bile acid and lipid excretion

Fecal samples (experiment 1) were obtained to determine fecal energy and bile acid (BA) excretion, as well as cholesterol and free fatty acid (FFA) excretion. Fecal energy excretion was calculated from the caloric content of approx. 300 mg dried feces samples using a Parr 6100 compensated calorimeter (Parr Instrument Company) and a 1108 Oxygen Bomb. Fecal BA excretion was assessed in dried feces samples (approx. 40–50 mg) by LC/MS as described before [24]. TC and FFA content was assessed in dried and pulverized feces samples (approx. 10–15 mg). Lipids were extracted with a mixture of 450 μL CH_3OH, 150 μL NaOH (10 M) and 150 μL H_2O by shaking at 600 rpm at 90 °C for 1 h. After cooling, 300 μL HCl (6 M) and 750 μL C_6H_{14} were added, samples were vortexed and centrifuged (1 min; 18,800 · g; room temperature), and 500 μL of the top layer was transferred and dried under a gentle stream of N_2. Samples were reconstituted in 100 μL 2% Triton X-100 in $CHCl_3$ and dried again to be reconstituted in 200 μL 2% Triton X-100 in H_2O and assayed for TC (11489232216; Roche Diagnostics) and FFAs (NEFA-HR(2); Wako).

2.10. Isolation of blood leukocytes and flow cytometry

Whole blood samples were diluted 1:1 in PBS and treated with erythrocyte lysis/fixation solution (349202; BD Biosciences) for 15 min at room temperature. After lysis, cells were pelleted by centrifugation (5 min; 596 · g; 4 °C) and washed 3 times with PBS. Isolated leukocytes were subsequently incubated with a cocktail of antibodies directed against CD3, CD11b, CD11c, CD19, CD36, CD45, CD62L, Ly6C, Ly6G, NK1.1, Siglec-F and TREML4 (details regarding the antibodies are presented in Table S4) in PBS supplemented with 0.5% BSA, 2 mM EDTA, True-Stain monocyte blocker (426103; Biolegend) and Brilliant Stain Buffer Plus (566385; BD Biosciences) for 30 min at 4 °C. Stained samples were analyzed by spectral flow cytometry using a Cytek Aurora Spectral flow cytometer (Cytek Biosciences). SpectroFlo v3.0 (Cytek Biosciences) was used for spectral unmixing of the flow cytometry data, and FlowJo™ v10.8 software (BD Biosciences) was used for gating of the data. A representative gating strategy is depicted in Supplementary Fig. S1A.

2.11. Hepatic VLDL-TG and VLDL-ApoB production rate

Mice (experiment 2) were anesthetized by intraperitoneal administration (10 mL · kg^{-1}) of a mixture of Acepromazin (0.63 mg · mL^{-1}), Midazolam (0.63 mg · mL^{-1}) and Fentanyl (0.03 mg · mL^{-1}), followed

by subcutaneous administration of 50 μL of the mixture if reflexes re-appeared (approx. every 45 min). Mice were intravenously injected with 10 μCi Tran[^{35}S] (IS-103; Hartmann Analytic) to label newly produced ApoB, and with 5 mL · kg^{-1} 10% Triton WR-1339 (T0307; Sigma-Aldrich) in PBS 30 min later to block lipoprotein lipase (LPL). Just prior to, and 15, 30, 60 and 90 min after injection with Triton WR-1339, blood was collected from the tail vein to measure TG accumulation in plasma as described above. 120 min after injection, mice were exsanguinated via the retroorbital sinus, and VLDL was isolated from serum by aspiration after density gradient ultracentrifugation at $d < 1.006$ g · mL^{-1} [25]. ^{35}S activity was determined by liquid scintillation counting (Ultima Gold, PerkinElmer as liquid scintillation cocktail; Tri-Carb 2910 TR, PerkinElmer as scintillation counter) in the VLDL fraction, before and after precipitation of ApoB with 2-propanol to calculate VLDL-ApoB production. VLDL-TG and VLDL-TC concentrations were determined as described above. The average size of the VLDL was determined by dynamic light-scattering using a fixed-angle Zetasizer Nano ZSP (Malvern Instruments).

2.12. Indirect calorimetry

Mice (experiment 3) were housed in indirect calorimetric home cages (Promethion Line; Sable Systems International). After two days of acclimatization, data on O_2 consumption (VO_2), CO_2 production (VCO_2) and voluntary locomotor activity (by beam breaks) were collected for five consecutive days. From the VO_2 and VCO_2, the respiratory exchange ratio and energy expenditure were calculated.

2.13. VLDL plasma decay and organ uptake

Mice (experiment 3) were intravenously injected with glycerol tri[^{3}H]oleate and [^{14}C]cholesteryl oleate double-labeled 80 nm-sized VLDL-like particles (1.0 mg TG in 200 μL PBS per mouse) prepared as described previously [26]. Blood was collected from the tail vein after 2, 5, 10, and 15 min to determine plasma decay. After 15 min, mice were killed by CO_2 inhalation and perfused via the heart with ice-cold PBS. Organs were collected and parts were dissolved in Solvable (PerkinElmer) at 56 °C overnight. Radioactivity was determined after addition of Ultima Gold (PerkinElmer) using a liquid scintillation counter (Tri-Carb 2910 TR; PerkinElmer). Plasma volume was estimated at 4.706% of total body weight and used to calculate total ^{3}H- and ^{14}C-activity in plasma [27]. Organ uptake of the radiolabels is expressed as a percentage of injected dose per gram wet tissue.

2.14. LPL activity assay

Snap-frozen interscapular brown adipose tissue (iBAT) and gonadal white adipose tissue (gWAT) samples (approx. 10–20 mg; experiment 3) were manually cut with a razor blade and incubated in DMEM (30 mg/mL; 31966, ThermoFisher Scientific) supplemented with 0.5% bovine serum albumin and 0.0004% heparin for 1 h at 37 °C. Samples were centrifuged (16.2 · *g*, 4 °C, 10 min), after which the middle layer containing heparin-bound LPL was collected to assess LPL activity *in vitro*. Thereto, 100 μL tissue extract was added to 200 μL substrate solution (9.2 mg/mL triolein (T7-140, Sigma), 6.7 μCi/mL [^{3}H]TO, 0.1% Triton X-100, 0.1 M Tris/HCl pH 8.6 (1.08382.100, Merck), 1% free FA-free bovine serum albumin (A6003, Sigma), and 20% heat-inactivated human serum). The reaction was stopped after 60 min by adding 3.25 mL of a mixture of heptane: methanol: chloroform (1 : 1.28: 1.37 v · v^{-1}) and K_2CO_3 (0.1 M), after which ^{3}H-activity was measured in the top layer following centrifugation (16.2 · *g*, 4 °C, 10 min), from which the TG hydrolase activity was calculated.

2.15. Statistical methods

Normality was confirmed by Shapiro Wilk tests, after which treatment effect was determined by two-way ANOVA and after Tukey *post-hoc* analysis. In cases where normality was not reached, the statistical interpretation was confirmed by a Kruskal–Wallis one-way ANOVA on ranks with Mann-Whitney U *post-hoc* analysis with Dunn-Sidak adjustment. Pearson product-moment correlation coefficients were used to determine VLDL-TG production rate. *p*-values less than 0.05 were considered statistically significant. Data are presented as mean ± SEM.

3. Results

3.1. Combined GIPR/GLP1R agonism lowers body weight by selectively reducing fat mass

Combined GIPR/GLP1R agonism administered every other day to Western-type diet-fed APOE*3-Leiden.CETP mice resulted in lower body weight throughout the intervention period when compared to vehicle treatment. After 10 weeks of treatment, mice that received the combined treatment showed an average body weight of 21.9 ± 0.8 g compared to 27.1 ± 0.4 g for vehicle treated mice (−19.3%; Fig. 1A), an effect explained by lower fat mass (2.7 ± 0.2 g *vs.* 7.0 ± 0.6 g, −62.3%; Fig. 1B) rather than a change in lean mass (Fig. 1C). The effect sizes of combined agonism were comparable to those of single GLP1R agonism, despite that GIPR agonism by itself also modestly reduced body weight (Fig. 1A) and fat mass (Fig. 1B). None of the treatments affected the cumulative caloric intake (Fig. 1D). In line with the reduction in total fat mass, combined GIPR/GLP1R agonism lowered the weight of iBAT, gWAT and subcutaneous (s)WAT, with effect sizes comparable to those observed by single GLP1R agonism (Fig. 1E–F). Single GIPR agonism also reduced gWAT and sWAT weight compared to vehicle, albeit to a lesser extent than single GLP1R and combined GIPR/GLP1R agonism (Fig. 1F). Furthermore, combined GIPR/GLP1R agonism lowered liver weight (−33%; Fig. 1G) accompanied by a pronounced reduction of hepatic TG (−45%), phospholipids (−29%) and TC (−34%) content when compared to vehicle treatment (Fig. 1H). Again these effects were comparable to those observed after treatment with the GLP1R agonist alone (Fig. 1G–H), while single GIPR agonism to a lesser extent also lowered liver weight (Fig. 1G) and reduced hepatic TGs (Fig. 1H). Expressing organ weights as percentage of total body weight resulted in comparable relative reductions of BAT, WAT and liver weights by the treatments (Supplementary Figs. S2A–C). These data indicate that both GIPR agonism and GLP1R agonism attenuate fat deposition in adipose tissue and in the liver. Overall, GLP1R agonism appeared more effective than GIPR agonism, and although none of the comparisons between single GLP1R agonism and combined GIPR/GLP1R agonism reached statistical significance in *post-hoc* analysis, combined agonism consistently performed slightly better than single GLP1R agonism.

3.2. Combined GIPR/GLP1R agonism attenuates atherosclerotic lesion severity

Atherosclerotic lesion size was determined in histological sections of the aortic root region, and lesion severity was scored by categorizing lesions as mild (type I-III) or severe (type IV-V) based on a grading system of the American Heart Association adapted for mice. Combined GIPR/GLP1R agonism non-significantly lowered lesion size when compared to vehicle treatment (−22%; Fig. 2A–B). In both single treatment groups, the number of mild and severe lesions was comparable (both 50%), and not statistically significantly different from vehicle treatment (Fig. 2C). Strikingly, the non-significantly reduced atherosclerotic lesion size upon combined GIPR/GLP1R agonism was accompanied by significantly attenuated atherosclerotic lesion severity as evidenced by a shift in the distribution of severe and mild lesions, from more severe than mild lesions (59% severe *vs.* 41% mild lesions) in vehicle treated mice to more mild than severe lesions (37% severe *vs.* 63% mild lesions) upon combined treatment (Fig. 2C). Next,

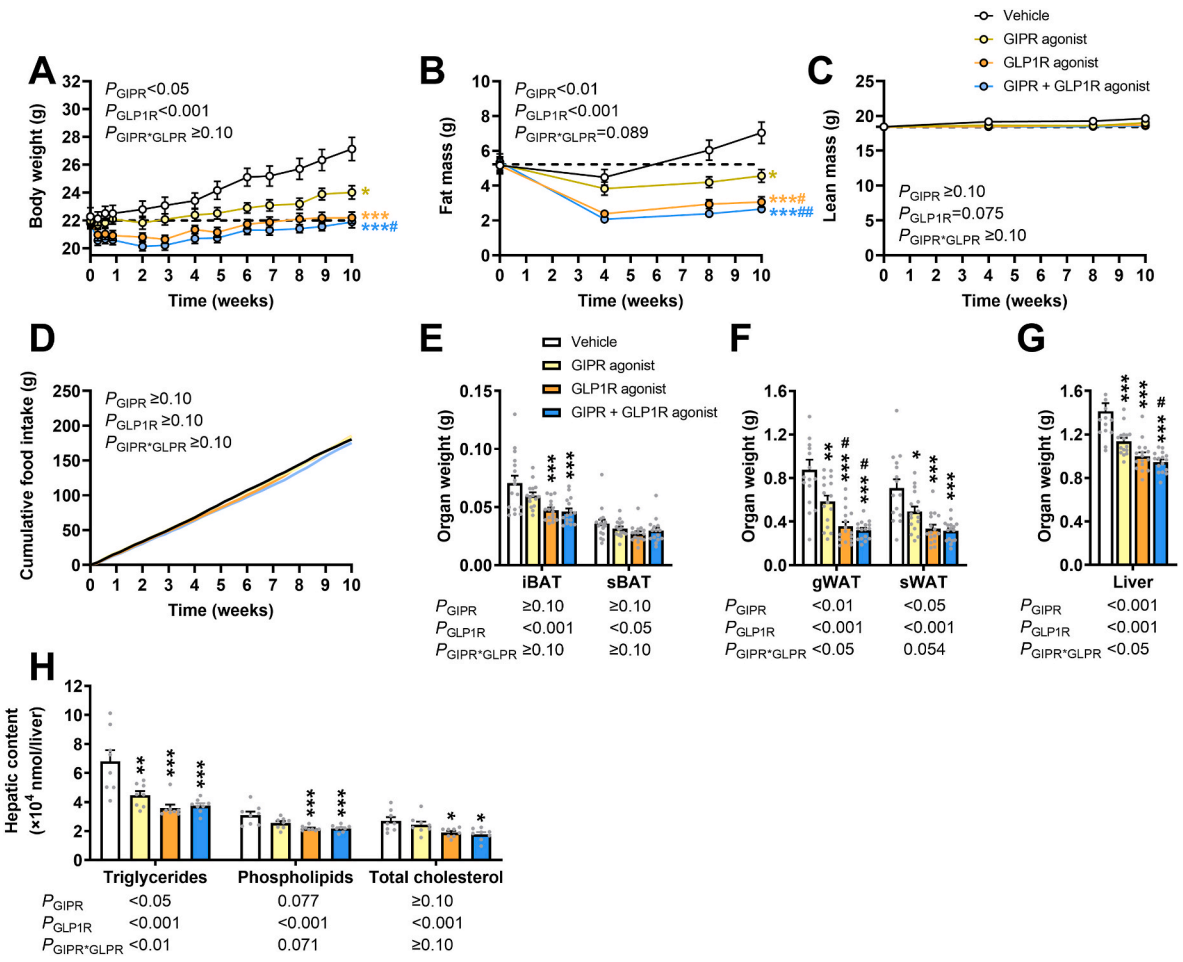

Fig. 1. Combined GIPR/GLP1R agonism lowers body weight by selectively reducing fat mass.
Female APOE*3-Leiden.CETP mice were fed a Western-type diet and received a subcutaneous injection with either a GIPR agonist (GIPFA-085; 300 nmol/kg), a GLP1R agonist (GLP-140; 30 nmol/kg), both agonists at these doses, or vehicle every other day. Throughout the intervention, (A) body weight, (B, C) body composition and (D) cumulative food intake were monitored. After 10 weeks of treatment, (E) interscapular and subscapular brown adipose tissue (iBAT; sBAT), (F) gonadal and subcutaneous white adipose tissue (gWAT; sWAT), and (G) liver weights were determined, and (H) hepatic lipid content was assessed. Data are presented as mean ± SEM and individual data points. A-C, E-G n=16 per group; D derived from n=4 cages per group, H n=8 per group. p-values of two-way ANOVA are depicted below the figure panels and symbols are used within figure panels for statistical differences identified by *post-hoc* analysis with $^{*}p < 0.05$, $^{**}p < 0.01$, $^{***}p < 0.001$ *vs.* vehicle and $^{\#}p < 0.05$, $^{\#\#}p < 0.01$ *vs.* GIPR agonism. (For interpretation of the references to color in this figure legend, the reader is referred to the Web version of this article.)

atherosclerotic plaque composition (*i.e.* smooth muscle cell, macrophage and collagen content) was determined within type III lesions, as they contain all of these lesion components. GLP1R agonism changed plaque composition according to the two-way ANOVA, characterized by increased macrophage and decreased collagen content (Fig. 2D–E). However, none of the treatment groups were significantly different from the vehicle group with regard to plaque composition in the *post-hoc* analysis. Taken together, these data suggest that atherosclerosis severity is attenuated only by the combined action of GIPR/GLP1R agonism.

3.3. GIPR and GLP1R agonism lower inflammatory state

We next investigated the effects of GIPR and GLP1R agonism on inflammation in the same APOE*3-Leiden.CETP mice. Combined GIPR/GLP1R agonism, but not the single treatments, attenuated the hepatic gene expression of the macrophage marker *F4/80* when compared to vehicle treatment (Fig. 3A). The monocyte and macrophage marker cluster of differentiation 68 (*Cd68*), as well as monocyte chemoattractant protein-1 (*Mcp-1*) were lowered upon combined GIPR/GLP1R treatment as explained by GLP1R agonism according to two-way ANOVA (Fig. 3A). Expression of tumor necrosis factor alpha (*Tnfa*) was lower in the combined treatment and single treatment groups when compared to vehicle treatment (Fig. 3A). Importantly, combined GIPR/GLP1R agonism lowered the circulating levels of the proatherogenic peptides ICAM-1 and VCAM-1, involved in binding of leukocytes to endothelial cells for transmigration (Fig. 3B). These effects were not significantly different from those observed in the single treatment groups (Fig. 3B). We next investigated whether the observed changes in hepatic expression of inflammatory markers and circulating levels of adhesion molecules might have translated into altered frequencies and activation status of circulating monocytes. To this end, we performed flow cytometry in blood drawn from APOE*3-Leiden.CETP mice that were treated daily with the agonists for two weeks. LY6C^{+} monocytes expressed as a fraction of CD45^{+} cells were not affected by the treatments, nor was the distribution over individual monocyte subsets (*i.e* conventional LY6C^{+} CD62L^{+}, intermediate LY6C^{+} TREML4^{+} or nonconventional LY6C^{low} CD62L^{-} CD11c^{+} monocytes; Fig. 3C). When expressed as number of cells per mL blood, the distribution over individual monocyte subsets was also not affected by the treatments (Supplementary Fig. S1B). According to the two-way ANOVA, GLP1R agonism lowered CD36 abundance in intermediate monocytes, and GIPR agonism lowered CD36 abundance in both the intermediate and

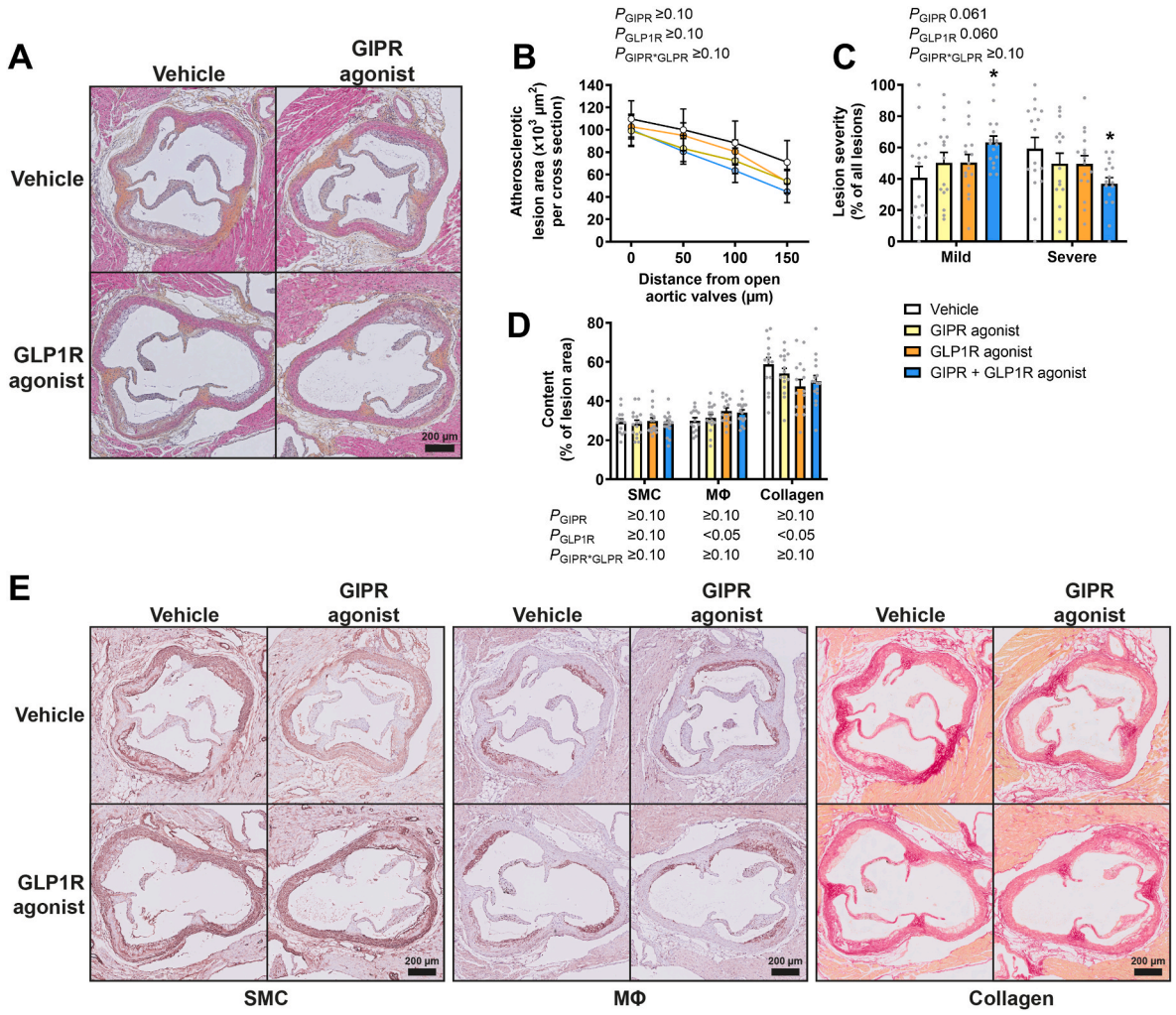

Fig. 2. Combined GIPR/GLP1R agonism attenuates atherosclerotic lesion severity.
Female APOE*3-Leiden.CETP mice were fed a Western-type diet and received a subcutaneous injection with either a GIPR agonist (GIPFA-085; 300 nmol/kg), a GLP1R agonist (GLP-140; 30 nmol/kg), both agonists at these doses, or vehicle every other day. After 10 weeks, hearts were collected and cross-sections of the aortic root area were stained with haematoxylin–phloxine–saffron, and (A) representative images are shown. (B) Atherosclerotic lesion area was determined and expressed as a function of distance from the appearance of open aortic valves. (C) Lesions were categorized according to lesion severity and expressed as a percentage of total lesions. (D) The smooth muscle cell (SMC, *i.e.* actin), macrophage (MΦ, *i.e.* MAC-3) and collagen (using Sirius Red) content were measured within type III lesions, and (E) representative images are shown. Data are presented as mean ± SEM and individual data points. n=16 per group. p-values of two-way ANOVA are depicted below the figure panels and symbols are used within figure panels for statistical differences identified by *post-hoc* analysis with $^*p < 0.05$ *vs.* vehicle. (For interpretation of the references to color in this figure legend, the reader is referred to the Web version of this article.)

nonconventional monocyte subsets (Fig. 3D). Significance for the single treatments was only reached for GIPR agonism in the nonconventional subset in *post-hoc* analysis. In contrast, combined GIPR/GLP1R agonism lowered the CD36 abundance in both the intermediate and nonconventional monocyte subsets when compared to vehicle treatment (Fig. 3D). Taken together, these data indicate that combined GLP1R/GIPR agonism in APOE*3-Leiden.CETP mice does not alter the frequencies of circulating monocyte subsets, but does lower their CD36 abundance.

3.4. *Combined GIPR/GLP1R agonism lowers plasma triglycerides without affecting circulating cholesterol levels*

To investigate whether combined GIPR/GLP1R agonism improved lipid and cholesterol metabolism, lipid levels were measured in plasma of the APOE*3-Leiden.CETP mice treated with vehicle, the GIPR agonist, the GLP1R agonist, or both agonists every other day. After 4 weeks of treatment, combined GIPR/GLP1R agonism lowered plasma TG levels compared to vehicle (−35%) while single GIPR and GLP1R agonism only non-significantly attenuated plasma TG levels (Fig. 4A). This reduction in plasma TGs upon combined GIPR/GLP1R agonism persisted throughout the intervention period. From week 8 of treatment onwards, the reduction in plasma TGs also reached statistical significance for single GLP1R agonism and after 10 weeks of treatment also for single GIPR agonism (Fig. 4A). The reduced overall TG level was reflected by both lowered TG levels within the VLDL and the IDL/LDL fractions as determined by FPLC profiling (Fig. 4E). However, despite this TG-lowering effect, plasma TC, HDL-C and non-HDL-C levels were not significantly affected by the treatments (Fig. 4B–D), nor were the cholesterol or phospholipid levels within the various lipoprotein fractions (Fig. 4F–G). We questioned whether a lowered total intestinal TG absorption may have contributed to the observed reduction in plasma TGs, and therefore measured fecal energy (Supplementary Fig. S2D) and FFA excretion (Supplementary Fig. S2E), but both were unaffected. Finally, we determined the effects of the agonists on plasma glucose and insulin levels after 10 weeks of treatment to find that both GIPR and GLP1R agonism lowered glucose levels without significantly affecting insulin levels (Fig. 4H–I). Overall, this led to a lowered HOMA-IR index

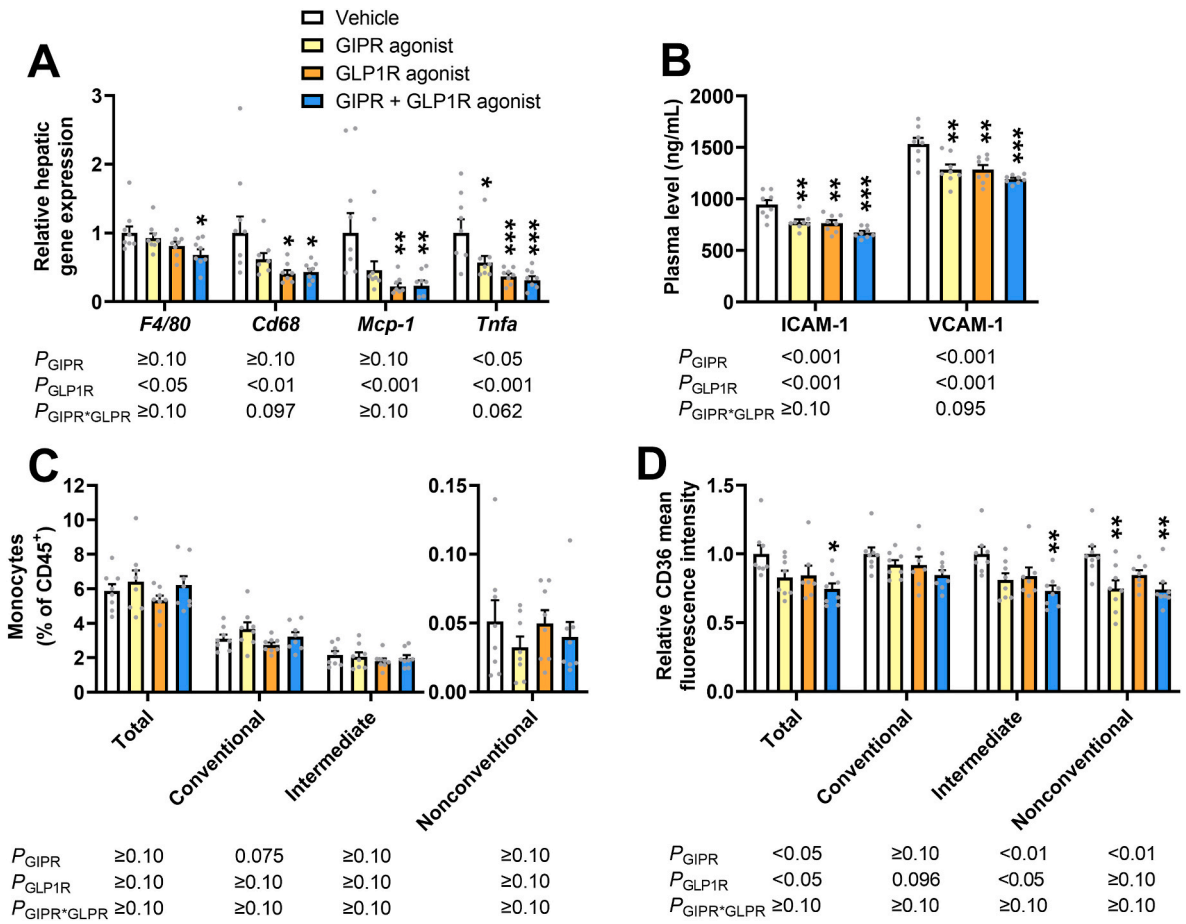

Fig. 3. GIPR and GLP1R agonism lowers inflammatory state.
Female APOE*3-Leiden.CETP mice were fed a Western-type diet and received a subcutaneous injection with either a GIPR agonist (GIPFA-085; 300 nmol/kg), a GLP1R agonist (GLP-140; 30 nmol/kg), both agonists at these doses, or vehicle every other day. (A) Hepatic gene expression levels of *F4/80*, cluster of differentiation (*Cd*)*68*, monocyte chemoattractant protein-1 (*Mcp-1*) and tumor necrosis factor alpha (*Tnfa*) were assessed. After 10 weeks of treatment, (B) circulating levels of intercellular adhesion molecule 1 (ICAM-1) and vascular cell adhesion protein 1 (VCAM-1) were determined in 4-h fasted blood. In a second experiment, mice were treated daily for 2 weeks on the same diet, unfasted blood was collected and (C) the frequency of monocytes (*i.e.* $LY6C^+$) as well as the frequency of conventional (*i.e.* $LY6C^+$ $CD62L^+$), intermediate (*i.e.* $LY6C^+$ $TREML4^+$) and nonconventional (*i.e.* $LY6C^{low}$ $CD62L^-$ $CD11c^+$) monocytes was determined by flow cytometry and expressed as a fraction of $CD45^+$ cells. (D) In these monocyte subsets, CD36 abundance was determined and expressed as mean fluorescence intensity relative to vehicle. Data are presented as mean ± SEM and individual data points. A-B n=16 per group; C-D n=8 per group. p-values of two-way ANOVA are depicted below the figure panels and symbols are used within figure panels for statistical differences identified by *post-hoc* analysis with $^*p < 0.05$, $^{**}p < 0.01$, $^{***}p < 0.001$ *vs.* vehicle.

as compared to vehicle (Fig. 4J).

3.5. Combined GIPR/GLP1R agonism increases VLDL-TG derived FA uptake by BAT and WAT, and increases VLDL remnant uptake by the liver

To investigate the mechanism behind the lowered plasma TG level upon combined GIPR/GLP1R agonism, another cohort of APOE*3-Leiden.CETP mice was treated daily with vehicle, the GLP1R agonist, the GIPR agonist or the combination thereof for 4 weeks. Combined GIPR/GLP1R agonism again caused an initial drop in body weight during the first week through a selective reduction in body fat mass (Supplementary Figs. S3A–C), and attenuated body weight gain in the following weeks, which resulted in lower adipose tissue and liver weights at end point when compared to vehicle-treated mice (Supplementary Figs. S3G–I). Respiratory quotient as measured by indirect calorimetry in the third week of treatment was not affected (Supplementary Fig. S3D), and GLP1R agonism modestly decreased total energy expenditure according to two way ANOVA (Supplementary Fig. S3E), likely explained by reduced total voluntary locomotor activity (Supplementary Fig. S3F). However, no significant differences could be identified in *post-hoc* analysis compared to vehicle. At the end of the 4 week treatment period, mice were injected with VLDL-like particles containing glycerol tri[^{3}H]oleate and [^{14}C]cholesteryl oleate to evaluate plasma clearance and organ uptake of TG-derived FAs and VLDL remnants, respectively. Combined GIPR/GLP1R agonism accelerated the plasma clearance of TGs compared to vehicle (Fig. 5A), which was explained by increased uptake of TG-derived FAs by iBAT (39.9% *vs.* 13.7% of the injected dose per gram tissue), sBAT (35.6% *vs.* 14.6% of the injected dose per gram tissue) and sWAT (4.6% *vs.* 2.3% of the injected dose per gram tissue) (Fig. 5B–C). Single GLP1R agonism also accelerated the clearance of TGs from the circulation, but only increased the uptake of TG-derived FAs by iBAT (Fig. 5B). Single GIPR agonism did not lead to significant changes in plasma clearance or organ uptake of TGs (Fig. 5A–C). The increase in lipolytic activity in iBAT upon combined GIPR/GLP1R agonism coincided with an increase in LPL TG-hydrolase activity (Supplementary Fig. S3J). Lipolytic activity in gWAT was unaffected, and so was LPL activity (Supplementary Fig. S3K). In accordance with the accelerated lipolytic processing of VLDL-like particles, combined GIPR/GLP1R agonism tended to accelerate the subsequent plasma clearance of VLDL remnants (Fig. 5D) primarily through increased hepatic uptake (38.5% *vs.* 23.0% of the injected dose per gram tissue; Fig. 5E). Both single treatments did not affect these parameters (Fig. 5D–E). The hepatic expression levels of the low-density lipoprotein receptor (*Ldlr*), the LDLr-related protein 1 (*Lrp1*)

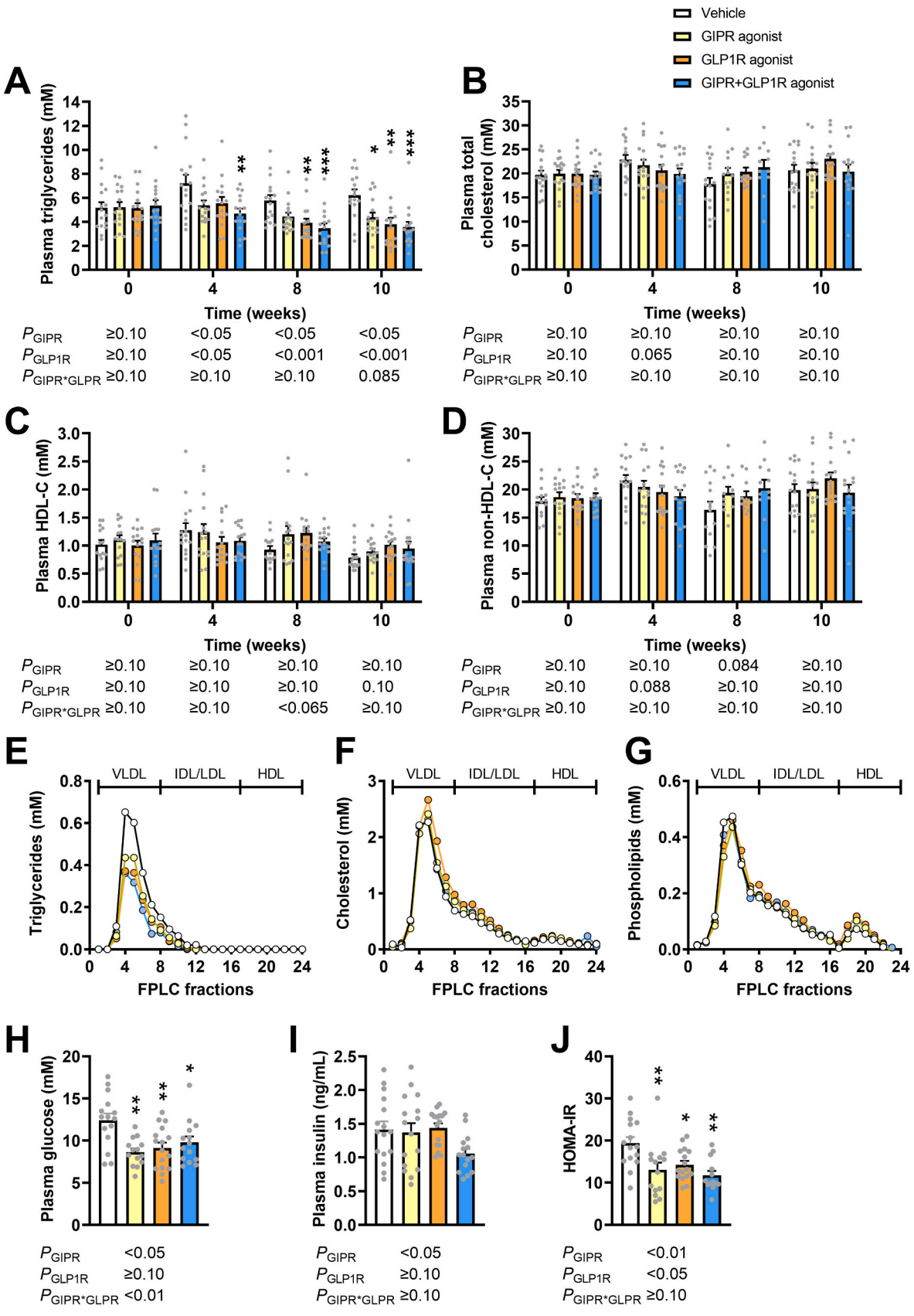

(caption on next page)

Fig. 4. Combined GIPR/GLP1R agonism lowers plasma triglycerides without significantly affecting circulating cholesterol levels.
Female APOE*3-Leiden.CETP mice were fed a Western-type diet and received a subcutaneous injection with either a GIPR agonist (GIPFA-085; 300 nmol/kg), a GLP1R agonist (GLP-140; 30 nmol/kg), both agonists at these doses, or vehicle every other day for 10 weeks. In 4-h fasted blood plasma samples, (A) triglycerides, (B) total cholesterol and (C) HDL-cholesterol were determined. (D) Non-HDL cholesterol was determined by subtracting HDL-cholesterol from total cholesterol. In pooled plasma samples collected 10 weeks after treatment, lipoprotein fractions were separated by fast protein liquid chromatography (FPLC) to measure (E) triglycerides, (F) cholesterol and (G) phospholipid levels per fraction. In 4 h fasted blood plasma samples collected after 10 weeks of treatment, (H) glucose and (I) insulin levels were determined, from which (J) the homeostatic model assessment for insulin resistance (HOMA-IR) was calculated. Data are presented as mean ± SEM and individual data points. n=16 per group. p-values of two-way ANOVA are depicted below the figure panels and symbols are used within figure panels for statistical differences identified by *post-hoc* analysis with $*p < 0.05$, $**p < 0.01$, $***p < 0.001$ *vs.* vehicle.

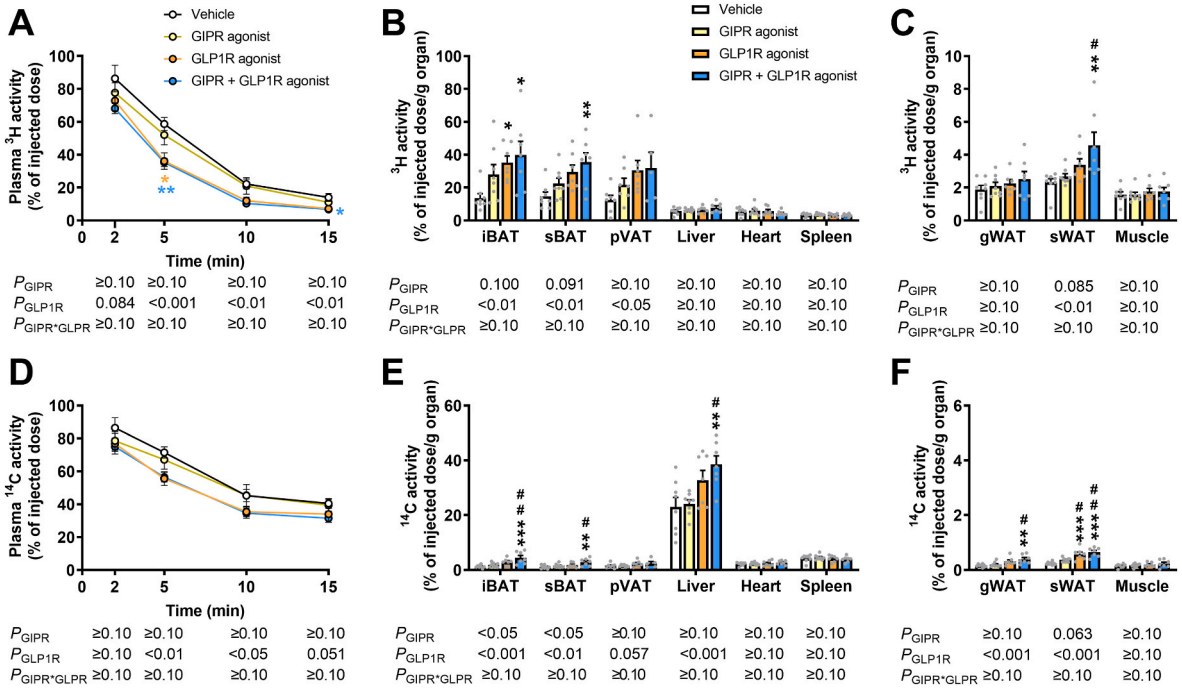

Fig. 5. Combined GIPR/GLP1R agonism increases VLDL-triglyceride derived fatty acid uptake by brown and white adipose tissue, and stimulates hepatic remnant clearance.
Female APOE*3-Leiden.CETP mice were fed a Western-type diet and received a daily subcutaneous injection with either a GIPR agonist (GIPFA-085; 300 nmol/kg), a GLP1R agonist (GLP-140; 30 nmol/kg), both agonists at these doses, or vehicle. After 4 weeks of treatment, plasma clearance and organ uptake of (A–C) triglyceride-derived ^{3}H-labeled fatty acids and (D–F) ^{14}C-labeled cholesteryl ester from recombinant VLDL-like particles were determined and expressed per gram interscapular and subscapular brown adipose tissue (iBAT; sBAT), perivascular adipose tissue (pVAT), liver, heart, spleen, gonadal and subcutaneous white adipose tissue (gWAT; sWAT), and muscle. Data are presented as mean ± SEM and individual data points. n=8 per group. p-values of two-way ANOVA are depicted below the figure panels and symbols are used within figure panels for statistical differences identified by *post-hoc* analysis with $*p < 0.05$, $**p < 0.01$, $***p < 0.001$ *vs.* vehicle and $^{\#}p < 0.05$, $^{\#\#}p < 0.01$ *vs.* GIPR agonism. (For interpretation of the references to color in this figure legend, the reader is referred to the Web version of this article.)

or N-deacetylase and N-sulfotransferase 1 (*Ndst1*), involved in the uptake of VLDL remnants, were not affected after 10 weeks of treatment (Supplementary Fig. S2F). The hepatic expression of angiopoietin-like 3 and 8 (*Angptl3*; *Angptl8*), encoding regulators of LPL activity, was also not affected (Supplementary Fig. S2G). Collectively, these data indicate that combined GIPR/GLP1R agonism increases the lipolytic activity of brown and white adipose tissues resulting in enhanced TG-derived FA uptake by these tissues, which is coupled to enhanced hepatic clearance of cholesterol-enriched VLDL remnants.

Previous studies have shown that during the lipolytic processing of TG-rich lipoproteins, surface remnants (mainly phospholipids) are sequestered into HDL to improve HDL's cholesterol efflux-inducing capacity from *e.g.* macrophages in atherosclerotic plaques, with subsequent esterification of the acquired cholesterol by lecithin–cholesterol acyltransferase (LCAT) and selective delivery of the cholesteryl esters to hepatocytes via scavenger receptor class B type 1 (SR-B1) [28,29]. We therefore measured the expression of ApoA1 (*Apoa1*), the major protein component of HDL, as well as LCAT (*Lcat*) and SR-B1 (*Scarb1*) in the livers of mice that were treated for 10 weeks with single or combined GIPR/GLP1R agonism. In addition, we measured the expression of ATP binding cassette subfamily A member 1 (*Abca1*) and ATP binding cassette subfamily G member 1 (*Abcg1*), involved in the assembly and maturation of HDL particles, respectively. However, besides a lower expression of *Abcg1* upon GIPR and GLP1R agonism compared to vehicle, the expression of these genes was not affected by the treatments (Supplementary Fig. S4), which is in line the unchanged HDL-C levels.

3.6. Combined GIPR/GLP1R agonism reduces hepatic VLDL-ApoB and VLDL-TG production

As the plasma TG level is also influenced by its hepatic production, we assessed *in vivo* hepatic VLDL-ApoB and VLDL-TG production rates after 4 weeks of treatment in the APOE*3-Leiden.CETP mice that were also used for flow cytometry. Combined GIPR/GLP1R agonism decreased the rate of VLDL-TG production (−33%) as well as VLDL-ApoB production (−33%), without affecting the average VLDL size (Fig. 6A–C). Interestingly, GLP1R agonism reached statistical significance in two-way ANOVA for the reduction in VLDL-TG production, while GIPR agonism reached significance for the reduced VLDL-ApoB production (Fig. 6A–B). GLP1R agonism modestly altered the relative

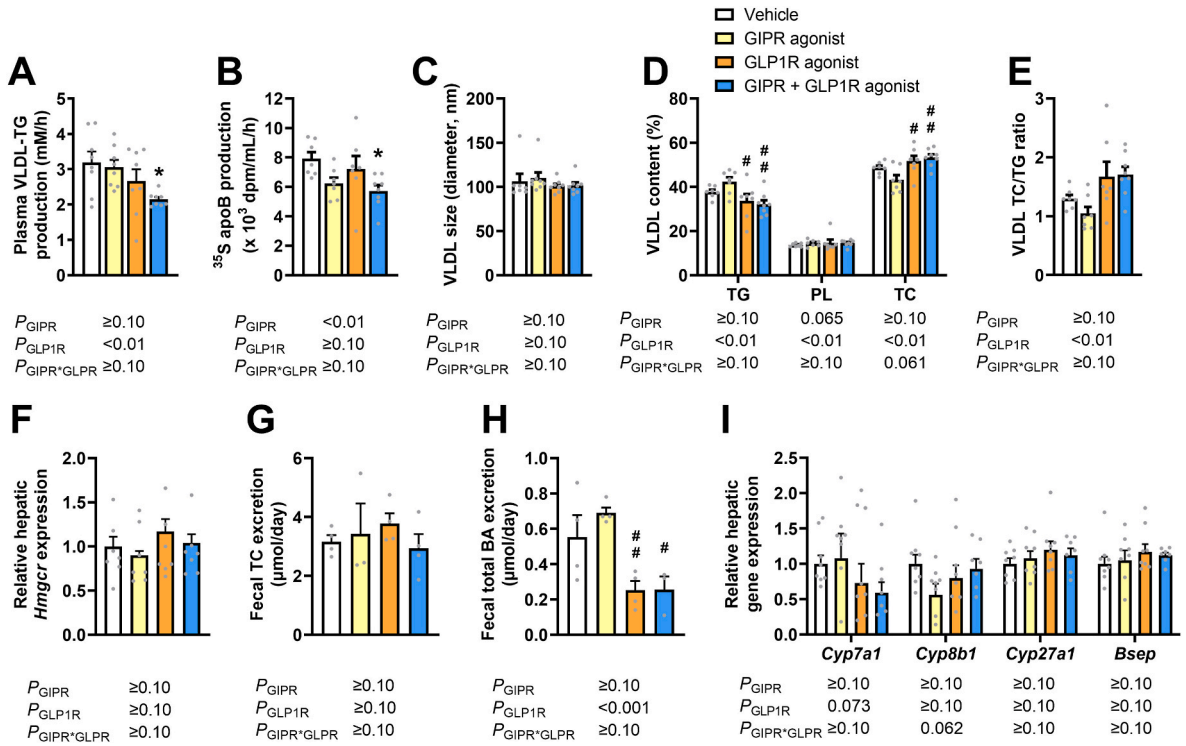

Fig. 6. Combined GIPR/GLP1R agonism reduces hepatic VLDL-ApoB and VLDL-TG production.
Female APOE*3-Leiden.CETP mice were fed a Western-type diet and received a daily subcutaneous injection with either a GIPR agonist (GIPFA-085; 300 nmol/kg), a GLP1R agonist (GLP-140; 30 nmol/kg), both agonists at these doses, or vehicle. After 4 weeks of treatment, mice received intravenous injection with Tran[^{35}S] label to label newly synthesized ApoB followed by Triton WR1339 to prevent lipolysis of VLDL. Plasma triglyceride (TG) levels were measured after 15, 30, 60 and 90 min, from which (A) VLDL-TG production rate was determined by linear regression. In isolated VLDL, (B) ^{35}S was measured to assess the production rate of newly synthesized ApoB. (C) VLDL size was determined by dynamic light-scattering, and (D) the relative contents of TGs, phospholipids (PL) and total cholesterol (TC) were assessed, from which (E) the TC/TG ratio was determined. In APOE*3-Leiden.CETP mice on the same Western-type diet treated every other day with vehicle or the same agonists for 10 weeks in total, (F) hepatic mRNA expression of 3-hydroxy-3-methylglutaryl-CoA reductase (*Hmgcr*) was assessed. (G) Fecal total cholesterol (TC) and (H) bile acid (BA) excretion was determined in samples collected from each home cage in the eighth week of intervention, and (I) hepatic mRNA expression of cholesterol 7 alpha-hydroxylase (*Cyp7a1*), sterol 12-alpha-hydroxylase (*Cyp8b1*), sterol 27-hydroxylase (*Cyp27a1*) and bile salt export protein (*Bsep*) was measured. Data are presented as mean ± SEM and individual data points. A-F, I n=8 per group; G-H derived from n=4 cages per group. p-values of two-way ANOVA are depicted below the figure panels and symbols are used within figure panels for statistical differences identified by *post-hoc* analysis with $^{*}p < 0.05$, $^{**}p < 0.01$, $^{***}p < 0.001$ *vs.* vehicle and $^{\#}p < 0.05$, $^{\#\#}p < 0.01$ *vs.* GIPR agonism.

VLDL content characterized by slightly lower TG, and higher phospholipid and TC content (Fig. 6D), resulting in an overall increased TC/TG ratio (Fig. 6E). Altogether we conclude that combined GIPR/GLP1R agonism primarily lowers VLDL particle production, while increasing the relative cholesterol content of VLDL, without affecting VLDL size.

Given the reduced VLDL production and accelerated VLDL clearance upon combined GIPR/GLP1R agonism, the question remained why plasma TC levels were unaffected. Therefore, we first measured expression of the rate-limiting enzyme in *de novo* cholesterol synthesis 3-hydroxy-3-methylglutaryl-CoA reductase (*Hmgcr*) in the livers of mice that were treated for 10 weeks with single or combined GIPR/GLP1R agonism, but these levels were unaltered (Fig. 6F). To investigate whether fecal cholesterol excretion was affected, feces samples were collected and analyzed. The treatments did not affect fecal cholesterol excretion (Fig. 6G). In contrast, concomitant GIPR/GLP1R agonism reduced the excretion of cholesterol as BAs as effected by GLP1R agonism according to two-way ANOVA (Fig. 6H). Significance compared to vehicle was not reached in *post-hoc* analysis, likely because fecal samples were collected from home cages with group-housed mice (*i.e.* n=4 per group). In the liver, expression of cholesterol 7 alpha-hydroxylase (*Cyp7a1*) and sterol 12-alpha-hydroxylase (*Cyp8b1*), involved in the classical BA synthesis pathway, and sterol 27-hydroxylase (*Cyp27a1*), involved in the alternative BA synthesis pathway, were not affected by the treatments, nor was expression of bile salt export protein (*Bsep*), involved in the biliary excretion of BAs (Fig. 6I). Overall, these data suggest that combined GIPR/GLP1R agonism lowers the fecal excretion of BAs with no evidence for altered *de novo* synthesis of cholesterol or production of BAs.

4. Discussion

Combined GIPR/GLP1R agonism is superior to single GLP1R agonism with respect to glycemic control and body weight loss in obese individuals with T2DM [10–12] and tirzepatide induces substantial weight loss in obese, non-diabetic participants when combined with lifestyle intervention (−22.5%, −23.6 kg; 72 weeks of intervention) [13]. The effects of combined GIPR/GLP1R agonism on asCVD are as of yet unknown. In the current study we show, by utilizing humanized APOE*3-Leiden.CETP mice, that combined GIPR/GLP1R agonism lowered markers of systemic inflammation and stimulated VLDL turnover, the combined action of which resulted in reduced atherosclerosis severity.

Whilst single GIPR or GLP1R agonism only resulted in non-significant improvements in atherosclerosis, we observed that combined GIPR/GLP1R agonism reduced lesion severity in APOE*3-Leiden.CETP mice, coinciding with lowered markers of systemic inflammation and a reduction in circulating TGs. Previous reports in ApoE and LDLr knockout mice did show attenuated atherosclerosis development upon single GIPR [30–32] or GLP1R [30,33–35] agonism, as mainly related to suppressed inflammatory responses. This seeming difference could in

theory be explained by the type and dosing of the single agonists. In the current study we attempted to mimic the imbalance of the GIPR and GLP1R agonist tirzepatide in the engagement with and activation of the GIPR *vs.* the GLP1R, with GIPR agonism predominating [36], rather than maximizing the effects of the individual agonists. The most likely explanation for the difference, however, is the choice of animal model. Atherosclerosis development in APOE*3-Leiden.CETP mice is primarily driven by circulating cholesterol levels [16] while atherosclerosis in cholesterol-fed ApoE and LDLr knockout mice is for a large part driven by inflammation. Nevertheless, we did observe that both single and combined treatment decreased ICAM-1 and VCAM-1 levels as markers for systemic inflammation in line with previous reports on single treatments [33,37–39]. Combined GIPR/GLP1R agonism additionally lowered CD36 levels within circulating monocytes. This is considered to be a biomarker for atherosclerotic lesion progression as positive associations have been found between *Cd36* expression in peripheral blood mononuclear cells and in the aortic wall where it stimulates inflammatory responses and foam cell formation [40,41]. While the expression of at least the GLP1R in various peripheral cell types is still a subject of debate [42], there is a general consensus that at least a proportion of endothelial cells and immune cells, including monocytes and macrophages, express both the GIPR [15] and the GLP1R [42]. The observed inflammatory changes may therefore be a direct result of engagement of the agonists with the receptors on those cells. Alternatively, there might be an indirect effect of decreased metabolic burden. Either way, the data are consistent with an anti-inflammatory role of combined GIPR/GLP1R agonism in improving atherosclerosis lesion severity.

In addition to attenuating systemic low-grade inflammation, combined GIPR/GLP1R agonism improved lipid metabolism, as evident by a striking and selective decrease in plasma TG levels. Mechanistically, we demonstrated that combined GIPR/GLP1R agonism both reduced hepatic VLDL-TG production and increased TG-derived FA uptake by BAT and WAT, without affecting TG uptake from the intestine. The lowered VLDL-TG production was paralleled by a similarly reduced ApoB production, indicating that combined GIPR/GLP1R agonism decreases VLDL particle production. The lowered VLDL-TG production was explained by GLP1R agonism, which is in line with our previous findings that single GLP1R agonism dose-dependently lowers VLDL-TG production in APOE*3-Leiden.CETP mice, as largely explained by reduced Srebp-1c-mediated lipogenesis [43]. Although in that study GLP1R agonism also lowered ApoB production, in the present study GIPR appeared critical for the decreased ApoB production as induced by combined GIPR/GLP1R agonism. In addition to lowering VLDL-TG production, GLP1R agonism was previously found to activate BAT and cause browning of WAT in mice [44]. Since the GLP1R is not expressed in adipocytes, these effects are likely due to sympathetic activation of these tissues [44]. In contrast, the GIPR is in fact present on adipocytes [45], and GIPR agonism may directly exert a dual action on the adipose tissue. Specifically, GIPR agonism increases both LPL expression and activity in human adipocytes [46,47] and stimulates fat deposition in WAT of human subjects [48]. At the same time, GIPR agonism enhances intracellular lipolysis by increasing cAMP production in murine white adipocytes [49,50]. The relative contribution of these opposing effects is most likely dependent on feeding status, with insulin overruling GIP's stimulatory effect on intracellular lipolysis [49,50]. Consequently, GIP improves the overall lipid-buffering capacity of WAT by accelerating lipid uptake in the postprandial state and promoting lipid excretion in the fasted state [1,11]. Considering that epidemiological studies have shown that TGs are a strong independent risk factor for asCVD [51], it is tempting to speculate that the reduction in plasma TGs is at least partly responsible for the beneficial effect of combined GIPR/GLP1R agonism on atherosclerosis. The underlying mechanism for this may be that TG-rich lipoproteins have a longer retention time within the intima of the arterial walls, allowing for more deposition of cholesterol, given that in absolute terms these particles contain up to 40 times more cholesterol per particle than LDL [52,53].

The enhanced delipidation of VLDL by the adipose tissues was coupled to an increased uptake of the generated VLDL remnants by the liver. This is likely dependent on ApoE-LDLr interaction that is fully functional in APOE*3-Leiden.CETP mice and is usually accompanied by a reduction in circulating cholesterol [16] and an increased hepatic excretion of BAs. However, in contrast to the large decrease in plasma TGs, GIPR/GLP1R agonism did not lower the circulating cholesterol level. We even observed a decrease in fecal BA excretion, but this did not affect fecal cholesterol excretion. As we also found no evidence for altered *de novo* synthesis of cholesterol, it is most likely that the lack of reduction of circulating cholesterol is caused by increased secretion of cholesterol from the liver within VLDL, in line with the observed higher TC/TG ratio within newly secreted VLDL particles.

Our data in APOE*3-Leiden.CETP mice are in line with GIPR and GLP1R agonism with NNC0090-2746 (RG7697) and tirzepatide in recent clinical phase 2 trials, showing reduced TG levels and a lesser effect on TC levels [10,11]. The recent phase 3 trial SURMOUNT-1 also showed that tirzepatide reduced TGs to a higher extent than TC [13]. Therefore, the effects of combined GIPR/GLP1R agonism on modulation of atherosclerosis in APOE*3-Leiden.CETP mice may well be predictive of the effects on human asCVD, similar to previous studies with classic pharmacological lipid-modulating strategies [54]. It is worth mentioning that in obesity, GIPR expression in WAT is downregulated and its signaling disrupted thereby affecting the lipid-buffering capacity of the tissue [55], an effect that can be efficiently restored upon weight loss [56]. Although we studied atherosclerosis development in relatively lean, female mice that are mostly protected against diet-induced obesity, GIPR agonism may thus be even more relevant in an obese context and exert even larger anti-atherogenic effects than observed in the current study. The ongoing phase 3 trial SURPASS-CVOT that investigates the effects of tirzepatide on major cardiovascular outcomes in obese individuals with T2DM (trial registration no. NCT04255433) will provide further insight. On a similar note, it would be of interest to investigate the effects of GIPR and GLP1R agonism on nonalcoholic fatty liver disease in the context of high-fat high-cholesterol diet-induced obesity.

In conclusion, combined GIPR/GLP1R agonism improves atherosclerotic lesion severity in dyslipidemic APOE*3-Leiden.CETP mice as explained by improvements in inflammation and increased VLDL turnover. Given that this mouse model is a well-established model for human lipoprotein metabolism and atherosclerosis development, we anticipate that combined GIPR/GLP1R agonism is also a promising strategy to lower cardiometabolic risk in humans. This hypothesis is currently tested with the SURPASS-CVOT phase 3 trial, comparing the effects of tirzepatide and the GLP1R agonist dulaglutide on major cardiovascular events in participants with T2DM.

Financial support

This work was supported by a grant from the Netherlands Cardio-Vascular Research Initiative: the Dutch Heart Foundation, Dutch Federation of University Medical Centers, the Netherlands Organization for Health Research and Development, and the Royal Netherlands Academy of Sciences [CVON-GENIUS-II] to P.C.N.R., a Lilly Research Award Program [LRAP] Award to P.C.N.R. and S.K., a Dutch Heart Foundation [2017T016] grant to S.K., and an NWO-VENI grant [09150161910073] to M.R.B.; J.F.D.B. is supported by the Nutrition and Health initiative of the University of Groningen; Z.Y. is supported by a full-time PhD scholarship from the China Scholarship Council.

Data availability

The datasets used and/or analyzed during the current study are available from the corresponding author on reasonable request.

CRediT authorship contribution statement

Robin van Eenige: Conceptualization, Formal analysis, Investigation, Writing – original draft, Writing – review & editing. **Zhixiong Ying:** Conceptualization, Formal analysis, Investigation, Writing – review & editing. **Naomi Tramper:** Formal analysis, Investigation. **Vera Wiebing:** Investigation. **Zohor Siraj:** Investigation. **Jan Freark de Boer:** Investigation. **Joost M. Lambooij:** Investigation. **Bruno Guigas:** Investigation. **Hongchang Qu:** Investigation. **Tamer Coskun:** Conceptualization, Investigation, Writing – review & editing. **Mariëtte R. Boon:** Writing – review & editing, Funding acquisition. **Patrick C.N. Rensen:** Conceptualization, Writing – review & editing, Funding acquisition. **Sander Kooijman:** Conceptualization, Investigation, Writing – review & editing, Supervision, Funding acquisition.

Declaration of competing interest

The authors declare the following financial interests/personal relationships which may be considered as potential competing interests: This work was also supported by a Lilly Research Award Program [LRAP] Award (to P.C.N.R. and S.K.). HQ and TC are employees and shareholders of Eli Lilly and Company. Eli Lilly and Company had no role in study design, data collection and analysis, decision to publish, or preparation of the manuscript.

Acknowledgments

The authors thank Amanda Pronk and Trea Streefland (Division of Endocrinology, Department of Medicine, LUMC, Leiden, The Netherlands), and Elsbet Pieterman (TNO-Metabolic Health Research, Gaubius Laboratory, Leiden, The Netherlands) for their excellent technical assistance. The graphical abstract was created with BioRender.com.

Appendix A. Supplementary data

Supplementary data to this article can be found online at https://doi.org/10.1016/j.atherosclerosis.2023.03.016.

References

[1] T.D. Muller, B. Finan, S.R. Bloom, et al., Glucagon-like peptide 1 (GLP-1), Mol. Metabol. 30 (2019) 72–130, https://doi.org/10.1016/j.molmet.2019.09.010.
[2] N.M. Krasner, Y. Ido, N.B. Ruderman, J.M. Cacicedo, Glucagon-like peptide-1 (GLP-1) analog liraglutide inhibits endothelial cell inflammation through a calcium and AMPK dependent mechanism, PLoS One 9 (2014), e97554, https://doi.org/10.1371/journal.pone.0097554.
[3] Y.-S. Lee, H.-S. Jun, Anti-inflammatory effects of GLP-1-based therapies beyond glucose control, Mediat. Inflamm. 2016 (2016), https://doi.org/10.1155/2016/3094642, 3094642-3094642.
[4] D.J. Drucker, Mechanisms of action and therapeutic application of glucagon-like peptide-1, Cell Metabol. 27 (2018) 740–756, https://doi.org/10.1016/j.cmet.2018.03.001.
[5] M. Jensterle, M. Rizzo, M. Haluzík, A. Janež, Efficacy of GLP-1 RA approved for weight Management in patients with or without diabetes: a narrative review, Adv. Ther. 39 (2022) 2452–2467, https://doi.org/10.1007/s12325-022-02153-x.
[6] A.E. Adriaenssens, E.K. Biggs, T. Darwish, et al., Glucose-dependent insulinotropic polypeptide receptor-expressing cells in the hypothalamus regulate food intake, Cell Metabol. 30 (2019) 987–996, https://doi.org/10.1016/j.cmet.2019.07.013, e986.
[7] P.A. Mroz, B. Finan, V. Gelfanov, et al., Optimized GIP analogs promote body weight lowering in mice through GIPR agonism not antagonism, Mol. Metabol. 20 (2019) 51–62, https://doi.org/10.1016/j.molmet.2018.12.001.
[8] R.J. Samms, M.P. Coghlan, K.W. Sloop, How may GIP enhance the therapeutic efficacy of GLP-1? Trends Endocrinol. Metabol. 31 (2020) 410–421, https://doi.org/10.1016/j.tem.2020.02.006.
[9] M.A. Nauck, E. Bartels, C. Orskov, R. Ebert, W. Creutzfeldt, Additive insulinotropic effects of exogenous synthetic human gastric inhibitory polypeptide and glucagon-like peptide-1-(7-36) amide infused at near-physiological insulinotropic hormone and glucose concentrations, J. Clin. Endocrinol. Metab. 76 (1993) 912–917, https://doi.org/10.1210/jcem.76.4.8473405.
[10] J.P. Frias, E.J. Bastyr 3rd, L. Vignati, et al., The sustained effects of a dual GIP/GLP-1 receptor agonist, NNC0090-2746, in patients with type 2 diabetes, Cell Metabol. 26 (2017) 343–352 e342, https://doi.org/10.1016/j.cmet.2017.07.011.
[11] J.P. Frias, M.A. Nauck, J. Van, et al., Efficacy and safety of LY3298176, a novel dual GIP and GLP-1 receptor agonist, in patients with type 2 diabetes: a randomised, placebo-controlled and active comparator-controlled phase 2 trial, Lancet 392 (2018) 2180–2193, https://doi.org/10.1016/S0140-6736(18)32260-8.
[12] J.P. Frias, M.A. Nauck, J. Van, et al., Efficacy and tolerability of tirzepatide, a dual glucose-dependent insulinotropic peptide and glucagon-like peptide-1 receptor agonist in patients with type 2 diabetes: a 12-week, randomized, double-blind, placebo-controlled study to evaluate different dose-escalation regimens, Diabetes Obes. Metabol. 22 (2020) 938–946, https://doi.org/10.1111/dom.13979.
[13] A.M. Jastreboff, L.J. Aronne, N.N. Ahmad, et al., Tirzepatide once weekly for the treatment of obesity, N. Engl. J. Med. (2022), https://doi.org/10.1056/NEJMoa2206038.
[14] A.-S. van Rijswijk, N. van Olst, W. Schats, D.L. van der Peet, A.W. van de Laar, What is weight loss after bariatric surgery expressed in percentage total weight loss (%TWL)? A systematic review, Obes. Surg. 31 (2021) 3833–3847, https://doi.org/10.1007/s11695-021-05394-x.
[15] Y. Mori, T. Matsui, T. Hirano, S.-i. Yamagishi, GIP as a potential therapeutic target for atherosclerotic cardiovascular disease–A systematic review, Int. J. Mol. Sci. 21 (2020), https://doi.org/10.3390/ijms21041509.
[16] J.F. Berbee, M.R. Boon, P.P. Khedoe, et al., Brown fat activation reduces hypercholesterolaemia and protects from atherosclerosis development, Nat. Commun. 6 (2015) 6356, https://doi.org/10.1038/ncomms7356.
[17] M. Westerterp, C.C. van der Hoogt, W. de Haan, et al., Cholesteryl ester transfer protein decreases high-density lipoprotein and severely aggravates atherosclerosis in APOE*3-Leiden mice, Arterioscler. Thromb. Vasc. Biol. 26 (2006) 2552–2559, https://doi.org/10.1161/01.ATV.0000243925.65265.3c.
[18] R. van Eenige, P.S. Verhave, P.J. Koemans, I. Tiebosch, P.C.N. Rensen, S. Kooijman, RandoMice, a novel, user-friendly randomization tool in animal research, PLoS One 15 (2020), e0237096, https://doi.org/10.1371/journal.pone.0237096.
[19] R.J. Samms, M.E. Christe, K.A.L. Collins, et al., GIPR agonism mediates weight-independent insulin sensitization by tirzepatide in obese mice, J. Clin. Investig. 131 (2021), https://doi.org/10.1172/JCI146353.
[20] T. Borner, C.E. Geisler, S.M. Fortin, et al., GIP receptor agonism attenuates GLP-1 receptor agonist–induced nausea and emesis in preclinical models, Diabetes 70 (2021) 2545–2553, https://doi.org/10.2337/db21-0459.
[21] E.G. Bligh, W.J. Dyer, A rapid method of total lipid extraction and purification, Can. J. Biochem. Physiol. 37 (1959) 911–917, https://doi.org/10.1139/o59-099.
[22] M.J. Gijbels, M. van der Cammen, L.J. van der Laan, et al., Progression and regression of atherosclerosis in APOE3-Leiden transgenic mice: an immunohistochemical study, Atherosclerosis 143 (1999) 15–25, https://doi.org/10.1016/s0021-9150(98)00263-9.
[23] M.C. Wong, J.A. van Diepen, L. Hu, et al., Hepatocyte-specific IKKbeta expression aggravates atherosclerosis development in APOE*3-Leiden mice, Atherosclerosis 220 (2012) 362–368, https://doi.org/10.1016/j.atherosclerosis.2011.06.055.
[24] R. van Eenige, Z. Ying, L. Tambyrajah, et al., Cannabinoid type 1 receptor inverse agonism attenuates dyslipidemia and atherosclerosis in APOE *3-Leiden.CETP mice, J. Lipid Res. 62 (2021), 100070, https://doi.org/10.1016/j.jlr.2021.100070.
[25] T.G. Redgrave, D.C. Roberts, C.E. West, Separation of plasma lipoproteins by density-gradient ultracentrifugation, Anal. Biochem. 65 (1975) 42–49, https://doi.org/10.1016/0003-2697(75)90488-1.
[26] P.C. Rensen, N. Herijgers, M.H. Netscher, S.C. Meskers, M. van Eck, T.J. van Berkel, Particle size determines the specificity of apolipoprotein E-containing triglyceride-rich emulsions for the LDL receptor versus hepatic remnant receptor in vivo, J. Lipid Res. 38 (1997) 1070–1084, https://doi.org/10.1016/S0022-2275(20)37190-X.
[27] M.C. Jong, P.C. Rensen, V.E. Dahlmans, H. van der Boom, T.J. van Berkel, L. M. Havekes, Apolipoprotein C-III deficiency accelerates triglyceride hydrolysis by lipoprotein lipase in wild-type and apoE knockout mice, J. Lipid Res. 42 (2001) 1578–1585, https://doi.org/10.1016/S0022-2275(20)32211-2.
[28] A. Bartelt, C. John, N. Schaltenberg, et al., Thermogenic adipocytes promote HDL turnover and reverse cholesterol transport, Nat. Commun. 8 (2017), 15010, https://doi.org/10.1038/ncomms15010.
[29] E. Zhou, Z. Li, H. Nakashima, et al., Hepatic scavenger receptor class B type 1 knockdown reduces atherosclerosis and enhances the antiatherosclerotic effect of Brown fat activation in APOE*3-Leiden, CETP Mice, Arteriosclerosis, thrombosis, and vascular biology 41 (2021) 1474–1486, https://doi.org/10.1161/ATVBAHA.121.315882.
[30] M. Nagashima, T. Watanabe, M. Terasaki, et al., Native incretins prevent the development of atherosclerotic lesions in apolipoprotein E knockout mice, Diabetologia 54 (2011) 2649–2659, https://doi.org/10.1007/s00125-011-2241-2.
[31] Y. Nogi, M. Nagashima, M. Terasaki, K. Nohtomi, T. Watanabe, T. Hirano, Glucose-dependent insulinotropic polypeptide prevents the progression of macrophage-driven atherosclerosis in diabetic apolipoprotein E-null mice, PLoS One 7 (2012), e35683, https://doi.org/10.1371/journal.pone.0035683.
[32] F. Kahles, A. Liberman, C. Halim, et al., The incretin hormone GIP is upregulated in patients with atherosclerosis and stabilizes plaques in ApoE(-/-) mice by blocking monocyte/macrophage activation, Mol. Metabol. 14 (2018) 150–157, https://doi.org/10.1016/j.molmet.2018.05.014.
[33] M. Arakawa, T. Mita, K. Azuma, et al., Inhibition of monocyte adhesion to endothelial cells and attenuation of atherosclerotic lesion by a glucagon-like peptide-1 receptor agonist, exendin-4, Diabetes 59 (2010) 1030–1037, https://doi.org/10.2337/db09-1694.

[34] G. Rakipovski, B. Rolin, J. Nøhr, et al., The GLP-1 analogs liraglutide and semaglutide reduce atherosclerosis in ApoE(-/-) and LDLr(-/-) mice by a mechanism that includes inflammatory pathways, JACC Basic Transl. Sci. 3 (2018) 844–857, https://doi.org/10.1016/j.jacbts.2018.09.004.
[35] J. Sanada, A. Obata, Y. Obata, et al., Dulaglutide exerts beneficial anti atherosclerotic effects in ApoE knockout mice with diabetes: the earlier, the better, Sci. Rep. 11 (2021) 1425, https://doi.org/10.1038/s41598-020-80894-x.
[36] T. Coskun, K.W. Sloop, C. Loghin, et al., LY3298176, a novel dual GIP and GLP-1 receptor agonist for the treatment of type 2 diabetes mellitus: from discovery to clinical proof of concept, Mol. Metabol. 18 (2018) 3–14, https://doi.org/10.1016/j.molmet.2018.09.009.
[37] H. Liu, A.E. Dear, L.B. Knudsen, R.W. Simpson, A long-acting glucagon-like peptide-1 analogue attenuates induction of plasminogen activator inhibitor type-1 and vascular adhesion molecules, J. Endocrinol. 201 (2009) 59–66, https://doi.org/10.1677/joe-08-0468.
[38] A. Ojima, T. Matsui, S. Maeda, M. Takeuchi, S. Yamagishi, Glucose-dependent insulinotropic polypeptide (GIP) inhibits signaling pathways of advanced glycation end products (AGEs) in endothelial cells via its antioxidative properties, Horm. Metab. Res. 44 (2012) 501–505, https://doi.org/10.1055/s-0032-1312595.
[39] J.M. Wilson, Y. Lin, M.J. Luo, et al., The dual glucose-dependent insulinotropic polypeptide and glucagon-like peptide-1 receptor agonist tirzepatide improves cardiovascular risk biomarkers in patients with type 2 diabetes: a post hoc analysis, Diabetes Obes. Metabol. 24 (2022) 148–153, https://doi.org/10.1111/dom.14553.
[40] L. Zhao, Z. Varghese, J.F. Moorhead, Y. Chen, X.Z. Ruan, CD36 and lipid metabolism in the evolution of atherosclerosis, Br. Med. Bull. 126 (2018) 101–112, https://doi.org/10.1093/bmb/ldy006.
[41] B. Yazgan, E. Sozen, B. Karademir, et al., CD36 expression in peripheral blood mononuclear cells reflects the onset of atherosclerosis, Biofactors 44 (2018) 588–596, https://doi.org/10.1002/biof.1372.
[42] B.A. McLean, C.K. Wong, J.E. Campbell, D.J. Hodson, S. Trapp, D.J. Drucker, Revisiting the complexity of GLP-1 action from sites of synthesis to receptor activation, Endocr. Rev. 42 (2021) 101–132, https://doi.org/10.1210/endrev/bnaa032.
[43] E.T. Parlevliet, Y. Wang, J.J. Geerling, et al., GLP-1 receptor activation inhibits VLDL production and reverses hepatic steatosis by decreasing hepatic lipogenesis in high-fat-fed APOE*3-Leiden mice, PLoS One 7 (2012), e49152, https://doi.org/10.1371/journal.pone.0049152.
[44] S. Kooijman, Y. Wang, E.T. Parlevliet, et al., Central GLP-1 receptor signalling accelerates plasma clearance of triacylglycerol and glucose by activating brown adipose tissue in mice, Diabetologia 58 (2015) 2637–2646, https://doi.org/10.1007/s00125-015-3727-0.
[45] R.E. Weaver, D. Donnelly, M. Wabitsch, P.J. Grant, A.J. Balmforth, Functional expression of glucose-dependent insulinotropic polypeptide receptors is coupled to differentiation in a human adipocyte model, Int. J. Obes. 32 (2008) 1705–1711, https://doi.org/10.1038/ijo.2008.148.
[46] S.J. Kim, C. Nian, C.H. McIntosh, Activation of lipoprotein lipase by glucose-dependent insulinotropic polypeptide in adipocytes. A role for a protein kinase B, LKB1, and AMP-activated protein kinase cascade, J. Biol. Chem. 282 (2007) 8557–8567, https://doi.org/10.1074/jbc.M609088200.
[47] S.J. Kim, C. Nian, C.H. McIntosh, GIP increases human adipocyte LPL expression through CREB and TORC2-mediated trans-activation of the LPL gene, J. Lipid Res. 51 (2010) 3145–3157, https://doi.org/10.1194/jlr.M006841.
[48] S.K. Thondam, C. Daousi, J.P.H. Wilding, et al., Glucose-dependent insulinotropic polypeptide promotes lipid deposition in subcutaneous adipocytes in obese type 2 diabetes patients: a maladaptive response, Am. J. Physiol. Endoc. M 312 (2017) E224–E233, https://doi.org/10.1152/ajpendo.00347.2016.
[49] C.H. McIntosh, I. Bremsak, F.C. Lynn, et al., Glucose-dependent insulinotropic polypeptide stimulation of lipolysis in differentiated 3T3-L1 cells: wortmannin-sensitive inhibition by insulin, Endocrinology 140 (1999) 398–404, https://doi.org/10.1210/endo.140.1.6464.
[50] L. Getty-Kaushik, D.H. Song, M.O. Boylan, B.E. Corkey, M.M. Wolfe, Glucose-dependent insulinotropic polypeptide modulates adipocyte lipolysis and reesterification, Obesity 14 (2006) 1124–1131, https://doi.org/10.1038/oby.2006.129.
[51] M.G. Levin, Remnant lipoproteins as a target for atherosclerosis risk reduction, Arterioscler. Thromb. Vasc. Biol. 41 (2021) 2076–2079, https://doi.org/10.1161/ATVBAHA.121.316341.
[52] J. Borén, K.J. Williams, The central role of arterial retention of cholesterol-rich apolipoprotein-B-containing lipoproteins in the pathogenesis of atherosclerosis: a triumph of simplicity, Curr. Opin. Lipidol. 27 (2016) 473–483, https://doi.org/10.1097/mol.0000000000000330.
[53] A.B. Wulff, B.G. Nordestgaard, Remnants and triglyceride-rich lipoproteins in prevention of premature coronary heart disease, Clin. Chem. 68 (2022) 266–268, https://doi.org/10.1093/clinchem/hvab241.
[54] S. Kühnast, M. Fiocco, J.W. van der Hoorn, H.M. Princen, J.W. Jukema, Innovative pharmaceutical interventions in cardiovascular disease: focusing on the contribution of non-HDL-C/LDL-C-lowering versus HDL-C-raising: a systematic review and meta-analysis of relevant preclinical studies and clinical trials, Eur. J. Pharmacol. 763 (2015) 48–63, https://doi.org/10.1016/j.ejphar.2015.03.089.
[55] V. Ceperuelo-Mallafre, X. Duran, G. Pachon, et al., Disruption of GIP/GIPR axis in human adipose tissue is linked to obesity and insulin resistance, J. Clin. Endocrinol. Metab. 99 (2014) E908–E919, https://doi.org/10.1210/jc.2013-3350.
[56] M. Asmar, N. Arngrim, L. Simonsen, et al., The blunted effect of glucose-dependent insulinotropic polypeptide in subcutaneous abdominal adipose tissue in obese subjects is partly reversed by weight loss, Nutr. Diabetes 6 (2016), https://doi.org/10.1038/nutd.2016.15 e208-e208.